Vol. 633: 37–54, 2020
https://doi.org/10.3354/meps13163

MARINE ECOLOGY PROGRESS SERIES
Mar Ecol Prog Ser

Published January 9

Predicting sediment organic carbon and related food web types from a physical oceanographic model on a subarctic shelf

James R. Lovvorn[1,*], Aariel R. Rocha[1], Seth L. Danielson[2], Lee W. Cooper[3], Jacqueline M. Grebmeier[3], Katherine S. Hedstrom[2]

[1]School of Biological Sciences, Southern Illinois University, Carbondale, IL 62903, USA
[2]College of Fisheries and Ocean Sciences, University of Alaska, Fairbanks, AK 99775, USA
[3]Chesapeake Biological Laboratory, University of Maryland Center for Environmental Science, Solomons, MD 20688, USA

ABSTRACT: In changing environments, conservation planning for bottom-feeding marine predators requires estimating the present and future spatial patterns of benthic communities. In the northern Bering Sea, we used the Regional Ocean Modeling System (ROMS) to hindcast near-bottom flows that redistribute settled phytodetritus and organic sediments, which in turn strongly affect the dispersion of 3 food web types that differentially favor spectacled eiders *Somateria fischeri*, walruses *Odobenus rosmarus*, or gray whales *Eschrichtius robustus*. Using data collected between 1994 and 2010, we interpolated spatial patterns of sediment organic carbon from field samples and correlated them with water depths and modeled flow velocities, temperatures, and salinities. In the deeper (mean 63 m) southern study area with weak net flows, hindcast near-bottom currents had negligible effects on patterns of sediment longer-term organic carbon (LTOC); instead, regional depth gradients and local bathymetry were the best predictors (r^2 = 0.72–0.85 among 7 years). In that area, climatic variations in total primary production would affect the areal extent of different LTOC levels, but not the core locations of persistent patches defined by depth. In the shallower (mean 39 m) northern study area with much faster flows, seafloor depth had negligible effects, and patterns of LTOC depended mainly on currents (r^2 = 0.48–0.55 over 2 years) that are subject to climatic changes in winds. Based on ranges of LTOC for different food web types, substantial portions of both areas must be conserved to ensure annual availability of all 3 types. Regional ocean circulation models driven by downscaled climate models provide important opportunities for projecting spatial patterns of key benthic habitats in this region.

KEY WORDS: Benthic assemblages · Benthic food webs · Sediment advection · Hydrographic models · Habitat delineation · Marine spatial planning

1. INTRODUCTION

At high northern latitudes, climate warming and global economic forces have encouraged expansion of oil and gas extraction, shipping, commercial fisheries, and other industrial development (Harris et al. 2018). Under these conditions, spatial planning for conservation requires estimating the present and future dispersion of high-value habitats and the food webs they support (Gormley et al. 2013, de la Torriente et al. 2019). Although particular species may drive commercial, legal, or subsistence concerns (Pautzke 2005, Lovvorn et al. 2015b, 2018b), conserving different habitats and food web support functions requires maintaining both diversity of taxa and their associated interactions in a changing climate (Kissling et al. 2012, Lovvorn et al. 2016). Because the present distributions of different taxa and their inter-

*Corresponding author: lovvorn@siu.edu

actions are expected to continue ongoing change, methods for tying food web structure and function to abiotic variables predicted by climate models would aid in long-term monitoring and spatial planning of conservation areas (Steenbeek et al. 2013, Hermann et al. 2016, Weinert et al. 2016). In this study, we evaluated a method for relating physical models of ocean bathymetry, flow velocity, temperature, and salinity to spatial patterns of the organic carbon content of surface sediments, a variable that is often a key determinant of benthic food webs.

The structure of benthic assemblages across marine landscapes has been correlated with diverse variables in different studies, and undoubtedly a range of variables interact to produce areas of high production by benthic food webs at large scales (e.g. Grebmeier et al. 2015a). However, it is usually not possible to protect entire regions from the joint effects of human impacts and climatic variations, and local patterns of food web types will vary within these broader regions. Regular monitoring to document the trajectories of diverse component taxa at high enough spatial resolution over large areas can be impractical because of high cost. One possible solution is to link the distributions of recognizable food web types to hydrographic models driven by physical variables that are more readily measured and modeled (Garcia et al. 2011). Efforts to relate the functioning of entire food webs to physical oceanographic models will be aided by variables that subsume diverse determinants of food web structure and function, as opposed to accounting for the individual responses of many biotic components to a range of environmental factors (McHenry et al. 2017).

As a single variable, the organic carbon (OC) content of surface sediments integrates many factors that regulate benthic assemblages. These factors include primary production and lateral advection of phytodetritus, larval dispersal and settlement, redox conditions, geochemical processes, and the relative effectiveness of filter- and deposit-feeding (reviewed by Lovvorn et al. 2018a). Sediment grain size is often a primary correlate of benthic assemblages, and is typically highly correlated with organic content (Grebmeier et al. 2015b, 2018, Lovvorn et al. 2018a). However, unlike sediment grain size, sediment OC functionally represents food inputs at the base of benthic food webs that modulate energy conveyed to higher trophic levels, thus altering assemblage structure and species interactions. As a result, in the northern Bering Sea, sediment OC is a powerful predictor of food web types as well as trajectories of change (Lovvorn et al. 2016, 2018a).

Over large areas of continental shelves in the Amerasian Arctic, soft sediments are dominated by deposit-feeders and filter-feeders that subsist mainly on settled microalgae (ice algae and phytoplankton) or on bacteria that consume algal-derived material (McTigue & Dunton 2014, North et al. 2014, Lovvorn et al. 2015a). For benthic macrofauna, food availability is generally more important than typical variations of temperature in regulating seasonal changes in metabolism and growth (Clarke 1988, Ahn et al. 2003, Carroll et al. 2009, Eriksson Wiklund et al. 2009). Deposit-feeders often depend largely on a longer-term 'food bank' of organic matter in sediments, apparently incorporated into and consumed as bacteria, regardless of the timing of major pulses of fresh phytodetritus (Mincks et al. 2008, McTigue & Dunton 2014, North et al. 2014). Accordingly, a number of analyses suggest that the OC content of surface sediments, often in conjunction with water depth, is frequently a good predictor of benthic biomass, assemblage structure, and food web function and their response to climatic changes (Denisenko et al. 2003, Grebmeier et al. 2006, 2015b, Gogina et al. 2010, Blanchard & Feder 2014, Lovvorn et al. 2016, 2018a).

At scales of tens of kilometers, spatial patterns of chlorophyll *a* in the underlying sediments often do not correspond to patterns of phytoplankton production in the upper water column (Lovvorn et al. 2013). Moreover, total sediment OC was not closely correlated ($r^2 = 0.22$) to surface sediment chlorophyll levels measured at certain times in the northern Bering and southern Chukchi Seas (Cooper et al. 2012, Grebmeier et al. 2018). These discrepancies likely result from asynchronous spatial patterns of initial settlement, followed by resuspension and lateral advection of phytodetritus which over time tends to accumulate in bathymetric depressions or regions of low flow (Puls & Sundermann 1990, Rutgers van der Loeff et al. 2002). Presumably due to shifts in advective regimes, longer-term studies have shown that the patch structure of sediment OC and related benthic assemblages can change over periods of decades to only a few years (Cooper et al. 2002, 2012, Lovvorn et al. 2014, Grebmeier et al. 2015b). However, the spatial and temporal scales at which sediment OC corresponds to local current patterns have not been investigated.

Identifying important habitats for marine birds and mammals is often an important priority in marine spatial planning (Lovvorn et al. 2014, 2015b, Citta et al. 2018). These highly mobile endotherms range over large areas seeking smaller patches of high prey density. Several large regions where benthic biomass is consistently high over time, referred to as 'hotspots' of

food web support to benthivorous top predators, have been identified in the northern Bering Sea (Grebmeier et al. 2015a). However, within those general areas are more localized patches of preferred prey types with high enough density to support profitable foraging. These subareas typically occupy only a fraction of the total area, and in some years can be quite restricted in size or in accessibility to air-breathing endotherms relative to ice cover (Nelson & Johnson 1987, Lovvorn et al. 2009, 2014, 2015b, Brower et al. 2017). Ensuring that such suitable patches are available in all years requires consideration of food web types at smaller scales (Blanchard & Feder 2014).

In the northern Bering Sea, different food web types associated with different ranges of sediment OC are more favorable to certain bottom-feeding predators owing to differing composition of major prey. For example, spectacled eiders *Somateria fischeri* prefer thin-shelled, deposit-feeding bivalves that are shallowly buried in muddy, highly organic sediments (Lovvorn et al. 2009, 2014); walruses *Odobenus rosmarus* often feed on thicker-shelled, facultative or filter-feeding bivalves buried deeper in less organic sediments (Oliver et al. 1983, Born et al. 2003, Sheffield & Grebmeier 2009); and gray whales *Eschrichtius robustus* typically focus on filter-feeding crustaceans in sandier sediments with lower OC (Oliver & Slattery 1985, Brower et al. 2017). These prey items are interdependent components of diverse assemblages which form recognizable food web types in different areas of the northern Bering Sea (Lovvorn et al. 2015a, 2016). Conservation planning to ensure availability of different food web types in all years would be aided by models that project the relative persistence of areas differing in sediment OC.

The Regional Ocean Modeling System (ROMS) is a 3-dimensional, time-explicit framework for modeling ocean and sea ice circulation. This framework has been adapted to a range of large marine systems including the Bering and Chukchi Seas (Curchitser et al. 2005, Danielson et al. 2011 and references therein). We used bathymetry, reanalysis winds, and ROMS model hindcasts of the near-bottom layer of the water column to relate seafloor depths, wind stress, current patterns, temperature, and salinity to the dispersion of sediment OC resulting from resuspension, lateral advection, and settling.

We analyzed model results within 2 regions of the northern Bering Sea having notably different advective regimes: south and offshore of St. Lawrence Island with only weakly directional flow fields, and the Chirikov Basin north of St. Lawrence Island with much stronger currents (Fig. 1; Clement et al. 2005, Danielson et al. 2014). Between 1994 and 2010, data on sediment OC and benthic assemblages were available from stations throughout these regions during 8 years in the southern area and 2 years in the northern area. We used these data to investigate the ability of

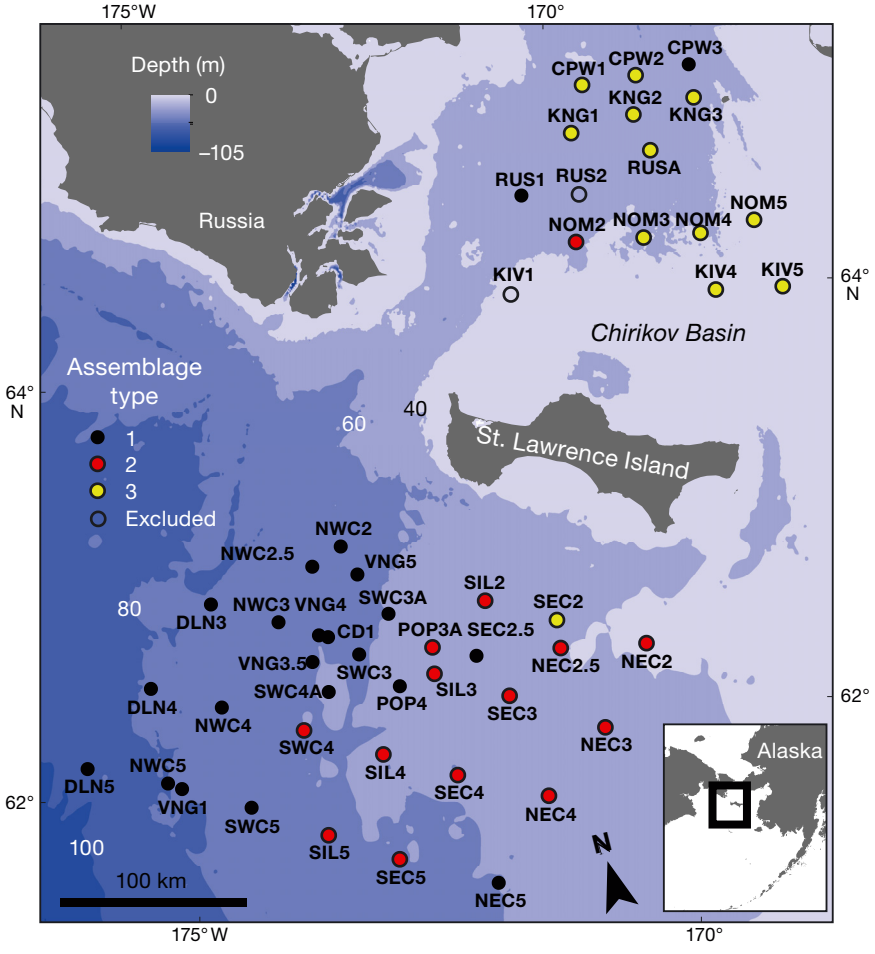

Fig. 1. Stations sampled for sediment non-algal organic carbon (OC; g C m^{-2}, excluding fresh microalgae) in the northern Bering Sea in May–June 2007, and bathymetry from the Alaska Region Digital Elevation Model v.2.0. Various combinations of these stations as well as others were sampled for sediment organic carbon in different years (Table 1). Stations shown were used in analyses of benthic assemblages, and station symbols are color coded for 3 main types of benthic assemblages and associated food webs (for details, see Section 2.3 and Lovvorn et al. 2018a)

the ocean circulation model to hindcast local areas of accumulation of sediment OC, and their relative persistence over multiple years. We then used these hindcasts to infer the location and extent of 3 major food web types associated with different levels of sediment OC, and the persistence of those distributions over time, in light of their differential food web support of spectacled eiders, walruses, and gray whales.

We began by performing regressions of observed sediment OC on a range of model output variables for each year separately, and compared the results to a regression based on all years combined. This comparison revealed whether there were variables important in only 1 or a few years that were not retained in the all-years regression, thus lessening the effectiveness of the all-years regression to predict the dispersion of sediment OC in those years. We also compared predictions from the all-years regression to observed sediment OC in each year to test the accuracy of predictions. We then used levels of sediment OC associated with 3 different food web types (Lovvorn et al. 2015a, 2018a) to delineate areas of these types based on regressions for each year and for all years combined. These analyses indicated the ability of the all-years regression to identify areas of the 3 types that would persist in all years, and how predictions would vary depending on the number of years of data used in the regressions. Comparison of predictions for individual years with predictions of 'average' conditions from the all-years regression was important to our goal of delineating areas that ensured adequate habitat availability even in years with extreme conditions. Competing human interests typically constrain the locations and extent of protected habitat to limited portions of average areas that are suitable. If the time series of available data subsumes extremes likely to occur in the foreseeable future, annual variations might be more suitable for planning than are longer-term averages, because they better capture the possible range of future conditions.

2. MATERIALS AND METHODS

2.1. Study area and sediment sampling

Water depths in our study area south of St. Lawrence Island ranged from 29 to 103 m (mean ± SD = 63 ± 15 m), and in the Chirikov Basin north of the island from 22 to 65 m (39 ± 9 m). During the period of this study (1994–2007), bottom water temperatures for much of the year were <0°C in the southern study area, and <2°C in the Chirikov Basin (higher during summer in eastern nearshore areas). In preceding decades and through the period of this study, this entire region was typically covered by pack ice for 5–6 mo per year. Bering Shelf Water dominates the area south of the island, with summer water and winter water characteristics (Danielson et al. 2017) evolving through the course of the year. South of St. Lawrence Island, there is persistent background flow toward the east in the nearshore zone (Danielson et al. 2006); however, in the offshore region of our study, the flow field exhibits modest current speeds without strong directional movement (Clement et al. 2005, Danielson et al. 2012). In the Chirikov Basin are 3 northward-flowing water masses, namely Anadyr Water, Bering Shelf Water, and Alaska Coastal Water positioned from west to east, respectively, which converge to pass through the Bering Strait at the northern end of the basin. These water masses differ substantially in temperature, salinity, and chemical characteristics (Danielson et al. 2017), and fronts between them shift seasonally and even by tens of kilometers in less than a week (Gawarkiewicz et al. 1994).

Sediments were sampled during cruises from mid-March to early June in 8 years between 1994 and 2010 (Table 1). A number of stations were the same among cruises, but various stations were added in different years. Fig. 1 shows stations at which benthic invertebrates and fish were sampled in 2006 and 2007, the years of data that were used to develop food web models for the region (Lovvorn et al. 2015a, 2016, 2018a).

At each station, we used the barrel of a syringe to collect duplicate 1 cm^3 sediment samples (1.54 cm^2

Table 1. Dates, cruise names, and numbers of stations sampled for organic carbon content of sediments in the northern Bering Sea south of St. Lawrence Island (SLI) and in the Chirikov Basin. Archived data for all cruises are available in Grebmeier & Cooper (2014, 2016)

Year	Days	No. of stations	Cruise name
South of SLI			
1994	26 May to 6 June	23	HX177
1999	13–27 April	32	PolarSea1999
2001	18 March to 1 April	35	PolarStar2001
2006	9 May to 2 June	60	HLY0601
2007	18–28 May	41	HLY0702
2008	16–23 March	20	HLY0801
2009	14–28 March	33	HLY0901
2010	13–29 March	44	PolarSea2010
Chirikov Basin			
2006	20–25 May	23	HLY0601
2007	29 May to 3 June	23	HLY0702

surface area) from the top of a van Veen grab before opening the grab. Total OC in samples acidified to remove inorganic carbonates was measured with a carbon-hydrogen-nitrogen analyzer (Control Equipment). Chlorophyll *a* (chl *a*) content of acetone-extracted samples was measured in accordance with Welschmeyer (1994) with a 10AU fluorometer (Turner Designs), and the 2 measurements were averaged (Cooper et al. 2002, 2012). (Surface sediment and chl *a* data are archived in Grebmeier & Cooper 2014, 2016) We converted chl *a* to g C of fresh microalgae by the ratio 34 g C (g chl *a*)$^{-1}$, which is representative of values during rapid growth (bloom) conditions reported for a variety of geographic areas (for review, see the Supplementary Material for Lovvorn et al. 2015a).

'Fresh' microalgae may include some chlorophyll that persists in sediments for long periods (Pirtle-Levy et al. 2009), but we are distinguishing intact algal cells containing viable chlorophyll from the more degraded, longer-term pool of organic matter in sediments. As both the Welschmeyer method and filters in the 10AU fluorometer mostly exclude breakdown products of chl *a* (e.g. pheophytin), our measurements were predominantly of chl *a* within microalgal cells that were still living or undegraded after recent settlement. The biomass of the pool of longer-term OC (LTOC) in sediments was calculated by subtracting fresh microalgal biomass (g C) from total OC. Spatial patterns of LTOC reflect net resuspension and redeposition of sediments on an annual basis, and its incorporation into bacteria appears to provide the main input to detritus-based food webs in this region (McTigue & Dunton 2014, North et al. 2014, Lovvorn et al. 2015a).

Earlier studies in this region showed that most biomass of infauna occurs within the top 5 cm (Grebmeier & McRoy 1989), and that sediments within that layer are usually well mixed (Pirtle-Levy et al. 2009). As LTOC concentrations change little to a depth of 5 cm, we extrapolated LTOC in the top 1 cm to the top 5 cm to represent its availability to most benthic macrofauna. Analyses of sediment samples in 1994 were not directly comparable to those in later years, so we used 1994 data to examine correlations within that year but not to evaluate the predictive capability of the subsequent reduced models.

2.2. Data analysis

The configuration of ROMS that we applied to this study covers a domain that extends from south of the Aleutian Islands to the North Atlantic on a telescoping grid, with 4–5 km horizontal resolution in the Bering Sea. We refer to this configuration as the Pan-Arctic ROMS (PAROMS). PAROMS has been implemented over 1983–2015 to compute the flow field, ice cover, and thermohaline conditions across 50 depth layers from the surface to the seafloor (Danielson et al. 2016). The model includes the underlying bathymetry and is driven by external forcing: wind stress, tides, earth rotation, surface heat and freshwater fluxes, and flows through the lateral boundaries. For a 50 m water column, the bottom layer in the model extends about 1.5 m above the seafloor.

We used PAROMS to characterize the bottom layer of the water column from 1994–2010, and computed monthly means of output fields. We examined near-bottom flow speed, the north–south flow velocity vector (V), the east–west flow velocity vector (U), salinity, and temperature. Tides, inertial currents, and other short-term flow variations were not explicitly considered in our analyses. We expected the monthly mean flow field to reflect mainly the influence of wind-driven motions and seasonal adjustments due to changes in the large-scale horizontal pressure gradients.

In addition to the model hindcasts, we also used data on surface winds and seafloor bathymetry. We obtained surface wind stress from the Blended Sea Winds data set (National Center for Environmental Information, https://www.ncdc.noaa.gov/data-access/marineocean-data/blended-global/blended-sea-winds). We used water depths having a horizontal resolution of about 1 km and a vertical resolution of 1 m from the Alaska Region Digital Elevation Model (ARDEM v. 2.0; Danielson et al. 2015).

To analyze bathymetry, wind, and PAROMS output within a GIS, we converted each variable from its original format into spatially referenced raster grids with Python v. 3.6 and Spyder (Scientific Python Development Environment, https://www.spyder-ide.org/). Using the Geospatial Data Abstraction Library (GDAL) 'numpy' and 'osgeo' modules (https://pypi.org/project/GDAL/), we applied the 'ReadAsArray' method to geotransform and project each array into geotiff format. Within ArcGIS, we converted the geotiffs into a polar stereographic equal-area projection, and resampled the PAROMS data from rectangular geographic cells (0.05° latitude × 0.2° longitude) into 4 square pixels (4.3 km × 4.3 km). Monthly mean data were summarized on several temporal scales (e.g. 5 yr mean, previous winter mean). We also created rasters for month-to-month changes in salinity, temperature, and currents.

Sediment transport models typically base erosion or deposition on a threshold of shear stress or flow speed

extrapolated via a logarithmic profile to the sediment surface from a flow speed measured or modeled some distance above the sea floor (Kösters & Winter 2014). However, such erosion thresholds vary substantially with sediment grain size, rugosity of the sea floor, effects of fauna on surface roughness and stability, and adhesion among particles due to biotic secretions (Thomsen & Flach 1997, Le Hir et al. 2007, Kösters & Winter 2014). Even with measurements of such effects, applying average values over large areas would misrepresent such heterogeneous processes at a range of spatial scales. In our initial attempts to predict accumulation of LTOC from near-bottom flows modeled by PAROMS, changing the threshold speed below which deposition should occur did not alter the accuracy of predicted patterns of LTOC relative to those measured by field sampling. Consequently, we relied on simple correlations of flow speeds in the bottom layer of PAROMS simulations with LTOC interpolated among sampling stations.

We used the 2007 sediment data south and north of St. Lawrence Island as a test case to explore spatial relationships between LTOC in surface sediments and possible correlates (Table A1 in the Appendix). In the statistical program R (version 3.44, with R packages 'car,' 'nlme,' and 'lme4'), we performed forward stepwise regression to identify independent variables that best predicted sediment LTOC. We used the variance inflation factor to identify the extent of multicollinearity between variables, and used Moran's I to identify spatial autocorrelation. Variables exhibiting these characteristics were not used in further analyses.

Based on results from analyses for 2007, we performed forward stepwise regressions with a reduced set of variables for all years (Table 2). As most variance in LTOC was explained by single variables in both the Chirikov Basin and south of St. Lawrence Island (see 'Results'), we then performed a geographically weighted regression (GWR) on LTOC for each year using that single best predictor variable (water depth for south of St. Lawrence Island, and north–south flow in certain months for the Chirikov region). GWR predicted the dependent variable (LTOC) from the independent variable (depth or north–south flow velocity) by a regression developed for each 1 km^2 pixel. The regression algorithm for each pixel included a variable number of neighboring stations (15 to 40) as selected by Akaike's information criterion corrected for small sample size (AIC_c), with closer locations carrying greater weight than more distant locations. Using predicted variables for each pixel, we produced a map of LTOC for each year. We then applied the thresholds of LTOC that distinguished 3 major food web types identified by Lovvorn et al. (2018a) to delineate the distributions of these types across the study area for each year.

2.3. Sediment organic carbon and food web types

Although benthic deposit-feeders in this region do ingest fresh microalgae, stable isotope and fatty acid biomarkers indicate that they assimilate mainly bacteria that consume well-reworked organic carbon (LTOC, McTigue & Dunton 2014, North et al. 2014; see also Mincks et al. 2008). (For food web models of carbon sources and flows, see Lovvorn et al. 2015a) Guided by these results, Lovvorn et al. (2018a) identified 3 major benthic food web types that occur along a gradient of levels of sediment LTOC in the northern Bering Sea. Type 1 is associated with high LTOC (>23 g C m^{-2} in the top 5 cm of sediments), and is a mainly deposit-feeding assemblage dominated by infaunal bivalves, polychaetes, nemerteans, sipunculids, priapulids, brittle stars, and flatfish. Type 3 is associated with relatively low LTOC (<9 g C m^{-2}) and has greater prevalence of filter-feeding bivalves and amphipods, as well as crabs, sea stars, and sculpins. Type 2 is intermediate between the other 2 types in LTOC and faunal composition, but with relatively higher bio-

Table 2. Independent variables regressed against longer-term organic carbon (LTOC) in sediments during all years of sampling (see Table 1). Winter was defined as October until the month of sampling (March, April, or May). PAROMS: Pan-Arctic Regional Ocean Modeling System

Bathymetric depth
Drainage area
Slope of sea floor, based on depths from PAROMS for each 19 km^2 pixel
Salinity (from PAROMS)
Individual means for each of the prior 12 mo
Mean and SD among all months during the prior 5 yr
Water temperature (from PAROMS)
Individual means for each of the prior 12 mo
Month-to-month change during the prior year
East–west and north–south flow vectors (from PAROMS)
Individual means for each of the prior 12 mo
Month-to-month change during the prior year
Mean and SD among all months during the current winter
Mean and SD among all months during the prior 5 winters
Resultant flow speed (from PAROMS)
Individual means for each of the prior 12 mo
Month-to-month change during the prior year

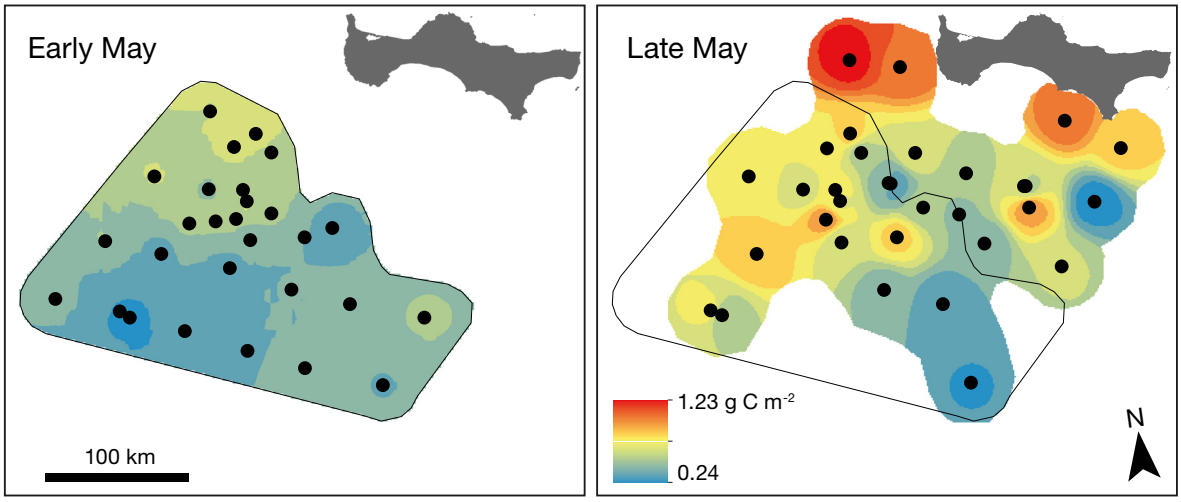

Fig. 2. Distribution of settled fresh microalgae in the top 1 cm of sediments south of St. Lawrence Island in the Bering Sea, 9–16 May vs. 17 May–2 June 2006. In late May, additional samples were taken outside the area represented by samples in early May (delineated for refrence in right panel)

mass of mussels (*Musculus* spp.) and whelks. Beyond the differences in food web structure (Lovvorn et al. 2015a), simulation modeling indicates that a number of the observed shifts in relative biomasses of different taxa can be induced by altering levels of sediment LTOC (Lovvorn et al. 2016). We applied the observed ranges of LTOC for the 3 food web types to the hindcast spatial patterns of LTOC to estimate the spatial patterns of these food web types in each year.

3. RESULTS

3.1. Longer-term sediment OC vs. fresh microalgae

The total OC content of surface sediments from March to early June (dates in Table 1) includes both recently settled fresh microalgae and the LTOC pool remaining at the end of winter. As seen south of St. Lawrence Island (Fig. 2), amounts and spatial patterns of settled microalgae vary tremendously over the course of the spring bloom, initial settling, and subsequent resuspension and advection. Thus, for a single field survey in a given year, patterns of fresh microalgae in the sediments will depend strongly on the timing of that survey relative to patterns of ice cover, phytoplankton bloom phenology, and subsequent wind and currents. Moreover, the spatial distribution of settled fresh microalgae can differ substantially from patterns for the longer-term OC pool, being almost opposite in some years such as 2007 and 2010 (Fig. 3). Because benthic assemblages include many organisms whose life histories encompass food availability over multiple seasons and years, we presumed that their spatial relationships with sediment OC are more accurately reflected in the longer-term pool that excludes recently settled (and still mobile) fresh microalgae. Thus, we restricted analyses to the longer-term pool (LTOC), which integrates resuspension, advection, and settlement of organic surface sediments over a year or more.

3.2. South of St. Lawrence Island

South and offshore of St. Lawrence Island, stepwise multiple regressions indicated that water depth was overwhelmingly the dominant and most consistent predictor of LTOC, explaining 65 to 76% of its variation in 8 years between 1994 and 2010 (Table 3). Far lower and less consistent annual influence was exerted by variation in east–west flow in March and April or the entire preceding winter of some years (3–11%), and by temperature changes from April to May or from month to month during October to February in some years (3–7%). The much higher correlation of LTOC with water depth than with current flows was consistent regardless of whether analyses considered mean flows during the month prior to sampling, during the entire preceding winter, or during the previous 5 winters. For all years combined, the regression showed similar dominance by depth with little to no effect of other variables (Table 3). (For all variables and years combined, the equation was LTOC = –34.1 + 1.0 [depth] + 362.3 [east–west flow in April], $r^2 = 0.77$, $p < 0.001$.)

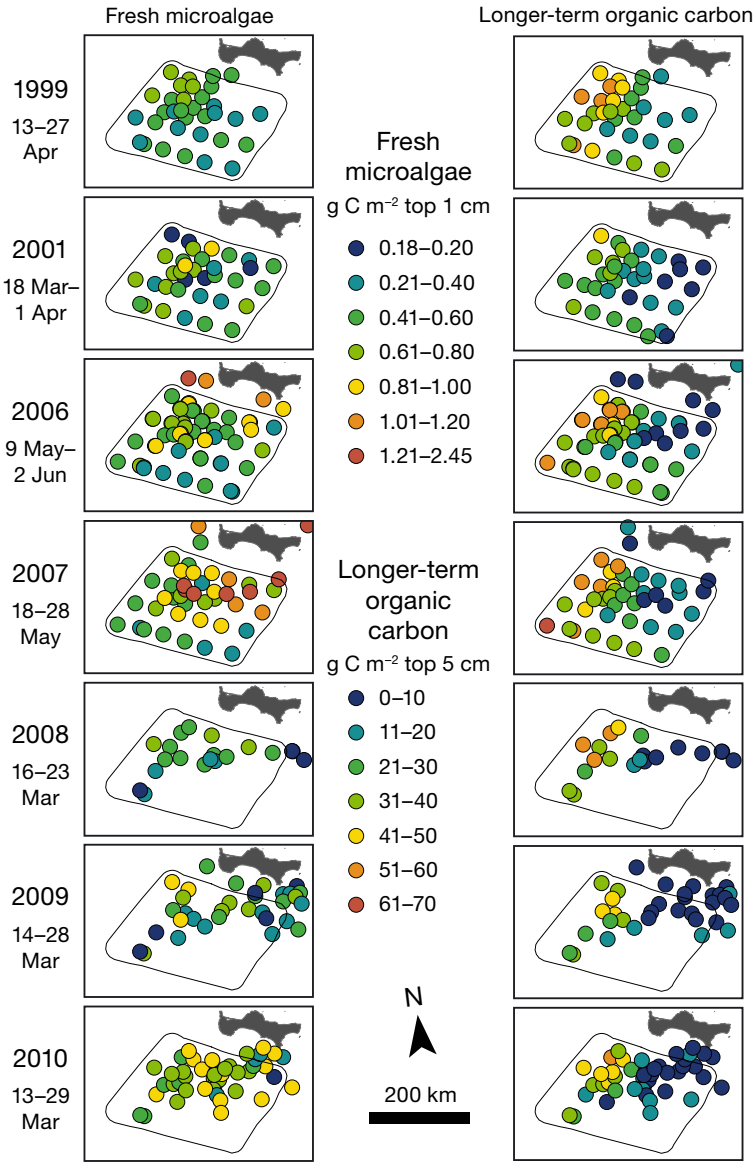

Fig. 3. Settled fresh microalgae and longer-term organic carbon (LTOC, excluding fresh microalgae) in sediments in different years south of St. Lawrence Island in the Bering Sea. The delineated area provides a spatial reference for varying locations of sampling stations

For each year, we used GWR (Gaussian kernel) to predict LTOC from water depth for each 1.0 × 1.0 km pixel. The resulting map of sediment OC showed a strong regional gradient with some scattered local patches of sediment accumulation (Fig. 4). Despite the modest net flow speeds in this area, the instantaneous flow field regularly exceeds 40 cm s^{-1} and is dominated by tides (which comprise about two-thirds of the total variance of instantaneous flow), with the largest semi-diurnal component (M_2) having a magnitude of nearly 16 cm s^{-1} (Danielson et al. 2012). Such a flow field can resuspend sediments intermittently. The over-arching process seems to be that once organic sediments are suspended by flows from any direction, they generally move downslope and tend not to flow back upslope, even in this region of very gradual depth gradients. LTOC is integrated over months to years, and appears to represent more the endpoint of the transport process (elevation) rather than variables affecting the rate or amount of sediment flowing transiently past any given point (slope, drainage area).

3.3. Chirikov Basin

Data on sediment OC and benthic organisms were available for the Chirikov Basin for 23 stations comprehensively sampled from 20–25 May 2006 and 29 May–3 June 2007 (Table 1). In this region, 3 water masses converge to flow northward through the narrow Bering Strait, resulting in mean monthly flow speeds from 1994–2010 that were generally 6.6 times greater in the Chirikov Basin (mean 6.6 cm s^{-1}, range 1.2–20.1 cm s^{-1}) than south of St. Lawrence Island (mean 1.0 cm s^{-1}, range 0.5–2.5 cm s^{-1}). Moreover, water depths were shallower in the Chirikov Basin (mean 39 m, range 22–65 m) than south of St. Lawrence Island (mean 63 m, range 29–103 m). Under these conditions of higher flows, shallower depths, and smaller range of depths in the Chirikov Basin, water depth had little effect on patterns of LTOC (Table 4). (For all variables and years combined, LTOC = –13.8 + 148.3 [north–south flow in December] – 14.2 [salinity change from Sep to Oct] + 0.5 [depth], $r^2 = 0.38$, $p < 0.001$). Instead, LTOC was best correlated with the speed of north–south flows in fall or early winter, and in 2007 on the variability of north–south flow speeds in the preceding 5 yr (Table 4). Salinity changes in early fall or spring, associated mainly with wind-driven shifts in relative positions of the major water masses (Gawarkiewicz et al. 1994), had relatively minor effects. Comparing the patterns of average surface wind stress during the same months in different years (Fig. 5) shows how very different the wind conditions can be, helping to explain why local resuspension and advection can overwhelm effects of depth or other variables in determining patterns of

Table 3. Partial and cumulative adjusted r^2 values for significant variables ($p < 0.05$) in stepwise regressions on longer-term organic carbon (LTOC) in the top 5 cm of sediments of the northern Bering Sea south of St. Lawrence Island. Correlations were positive unless indicated as negative (–). Positive north–south flow is northward, and positive east–west flow is eastward. However, a positive correlation indicates the direction of relationship between variables such that a negative correlation could signify a lessening of positive (northward) flow. Regression equations for depth (*D*) alone are provided for each year and for all years combined (all $p < 0.001$)

Year	Variable	Partial r^2	Cumulative r^2	
1994	Depth (LTOC = –47.0 + 1.06 *D*)		0.74	
	East–west flow in Mar 1994	0.10	0.84	
	Temperature change, Apr to May 1994	0.03	0.87	
	Temperature change, Oct to Nov 1993	0.03	0.90	
1999	Depth (LTOC = –34.8 + 1.05 *D*)		0.65	
	Temperature in Dec 1998	0.07	0.72	
2001	Depth (LTOC = –27.5 + 0.8 *D*)		0.68	
	Temperature change, Dec 2000 to Jan 2001	0.06	0.74	
	Temperature in Apr 2000	0.03	0.77	(–)
2006	Depth (LTOC = –31.0 + 0.9 *D*)		0.69	
	East–west flow in Apr 2006	0.11	0.80	
	Temperature change, Feb to Mar 2006	0.04	0.84	(–)
	Resultant flow speed in Mar 2006	0.01	0.85	(–)
2007	Depth (LTOC = –38.8 + 1.1 *D*)		0.74	
	East–west flow in Apr 2007	0.06	0.80	
	Change in resultant flow speed, Dec 2006 to Jan 2007	0.03	0.83	(–)
2008	Depth (LTOC = –34.1 = 1.0 *D*)		0.76	
	Temperature in May 2007	0.13	0.89	
2009	Depth (LTOC = –30.5 + 0.9 *D*)		0.75	
	Temperature change, Apr to May 2008	0.04	0.79	
	East–west flow (prior winter mean)	0.03	0.82	
	Temperature in Mar 2009	0.03	0.85	(–)
2010	Depth (LTOC = –34.1 + 1.0 *D*)		0.68	
	North-south flow in Mar 2010	0.07	0.75	
	Temperature change, Nov to Dec 2009	0.04	0.79	
	Temperature change, Jan to Feb 2010	0.07	0.86	(–)
	Slope	0.02	0.88	
	Resultant flow speed in Jun 2009	0.02	0.90	(–)
All years	Depth (LTOC = –34.4 + 1.0 *D*)		0.72	
	East–west flow in April	0.05	0.77	

sediment OC in this area. Large but spatially coherent variations in monthly means of north–south flow speed among years and seasons (Fig. 6) further attest to the importance of the variability of wind-driven currents in this region.

However, the particular months in which winds and associated water-mass positions (salinity) exerted their effects varied substantially between the 2 years of sampling (Table 4). Moreover, except for 2 stations, the range of levels of LTOC in the Chirikov Basin was far less than south of St. Lawrence Island (1–30 vs. 1–70 g C m^{-2}, cf. Figs. 4 & 7), thereby reducing the scope of values for developing predictive models. As a result, the regression for both years combined was strongly influenced by a small northeastern region with unusually high LTOC in 2007, and thus yielded high predictive capability in 2007 (r^2 = 0.60) but less so in 2006 (r^2 = 0.18; Fig. 7). When the timing of flows from the same year was used in the absence of the northeastern concentration of LTOC, the correlation in 2006 was much higher (r^2 = 0.48, Table 4). In practice, such inconsistencies could be anticipated based on longer-term physical data, which indicated large annual differences in the timing, direction, and magnitude of winds (Figs. 5 & 6). In such cases, modeling patterns of LTOC will require longer time series of sediment sampling to subsume the range of annual variability in winds and LTOC patterns.

3.4. Mapping predicted food web types

Based on food web types associated with differing ranges of LTOC (see Section 2.3), we evaluated the relative persistence of regions with different food web types as predicted from the regression models for LTOC in the Chirikov Basin and the area south of St. Lawrence Island (cf. Steenbeek et al. 2013). South of St. Lawrence Island, conditions favoring the mainly deposit-feeding assemblage dominated by infaunal bivalves, various worm taxa, brittle stars, and flatfish (Type 1) occupied a consistently large area in the 7 years sampled between 1999 and 2010 (Fig. 8). However, the extent of assemblage Type 3, with a greater prevalence of filter-feeding bivalves, amphipods, crabs, sea stars, and sculpins, ranged from quite limited in 1999 and 2006 to much greater in 2008–2010. The extent of the intermediate Type 2 assemblage also varied substantially, but not as much as Type 3. Bathymetry, the variable from which the relative extents of LTOC in different years were estimated in this region, did not show such annual variations. Thus, varying amounts of organic inputs among years modulated the areal extent of different LTOC levels, but not the core locations of persistent patches defined by depth.

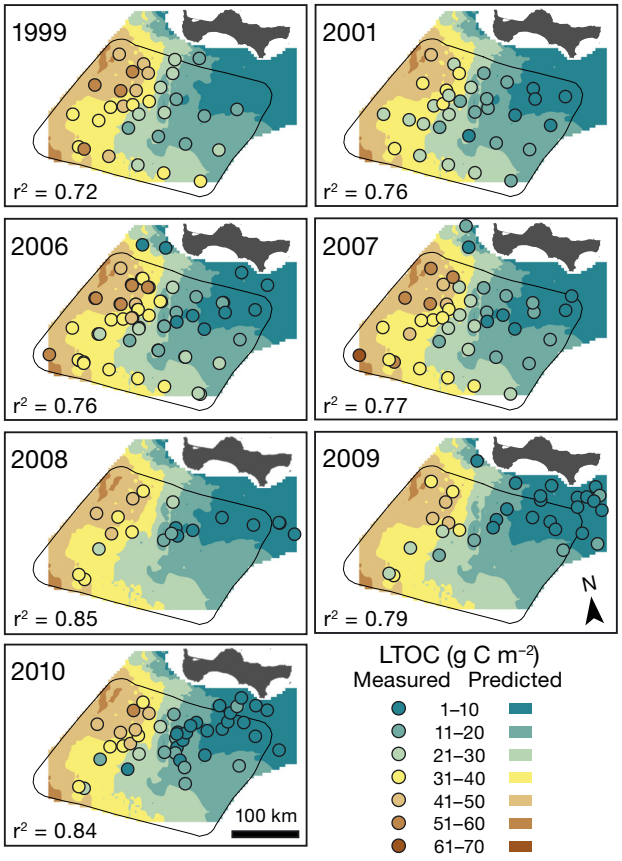

Fig. 4. Longer-term organic carbon (LTOC, excluding fresh microalgae, g C m^{-2}) in the top 5 cm of sediments measured at sampling stations (circles), relative to LTOC predicted from water depth for each 1 km^2 pixel by geographically weighted regression (GWR) for all years combined (equation for all years in Table 3). Annotated r^2 values are from linear regressions of values predicted vs. observed at each station

Table 4. Partial and cumulative adjusted r^2 values for significant variables ($p < 0.05$) in stepwise regressions on longer-term organic carbon (LTOC) in the top 5 cm of sediments in the Chirikov Basin region of the Bering Sea north of St. Lawrence Island. Conventions as in Table 3. Regression equations for north–south flow (F) alone are provided for each year and for both years combined (all $p < 0.001$)

Year	Variable	Partial r^2	Cumulative r^2	
2006	North–south flow in Sep 2005 (LTOC = 0.5 + 143.3 F_{Sep05})		0.48	
	Salinity change, Sep to Oct 2005	0.10	0.58	(–)
2007	North–south flow in Dec 2006 (LTOC = 3.1 + 404.3 F_{Dec06})		0.55	
	North–south flow SD, 2002 to 2007	0.17	0.72	(–)
	Salinity change, May to Jun 2006	0.04	0.76	
Both years	North–south flow in Dec (LTOC = 5.4 + 228.4 F_{Dec})		0.28	
	Change in salinity, Sep to Oct	0.05	0.33	(–)
	Depth	0.05	0.38	

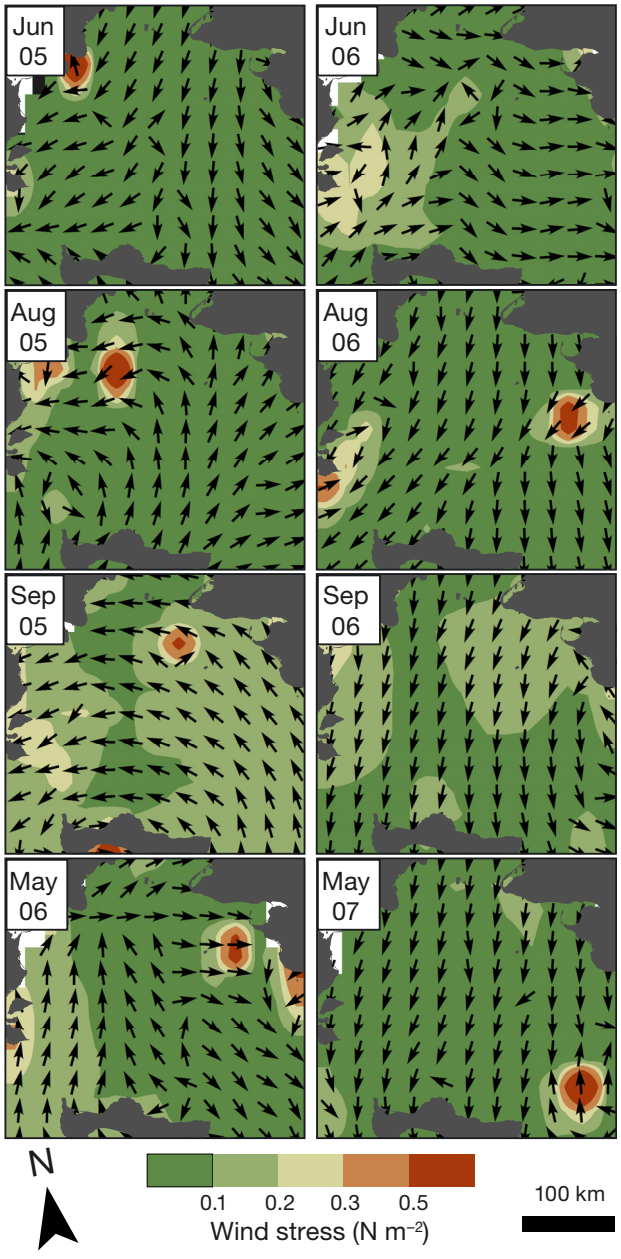

Fig. 5. Mean surface wind stress (N m^{-2}) in the Chirikov Basin in selected months, 2005–2007

In the Chirikov Basin, the spatial distribution of predicted food web types was quite different, with higher current speeds and shallower and less varied water depths leading to greater extent of assemblage Type 3 associated with lower sediment OC (Fig. 9). More depositional conditions favoring food web Type 1 occurred only in the northern portion and in only 1 of 2 years of sampling. Conditions favoring the intermediate Type 2 occurred in the southeast central and northern portions of the Chirikov Basin.

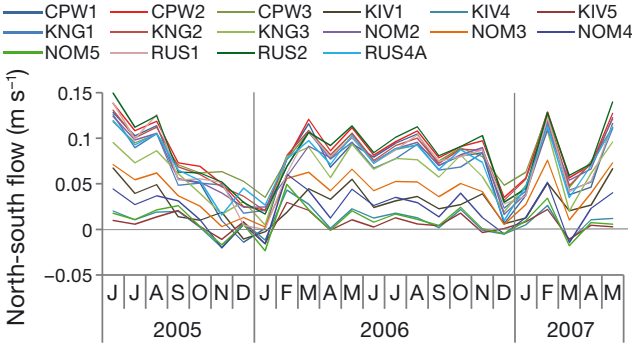

Fig. 6. Time series of north–south flow speed (m s^{-1}) over different stations (see Fig. 1 for locations) in the Chirikov Basin in different months and years. Positive (negative) values indicate northward (southward) flow

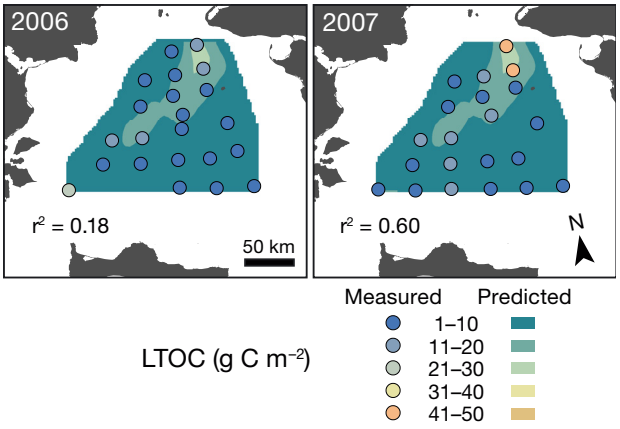

Fig. 7. Longer-term organic carbon (LTOC, excluding fresh microalgae, g C m^{-2}) in the top 5 cm of sediments at sampling stations (circles), relative to LTOC predicted from north–south flow in December for each 1 km^2 pixel by geographically weighted regression (GWR) for both years combined (equation for all years in Table 4). Annotated r^2 are from linear regressions of values predicted vs. observed at each station

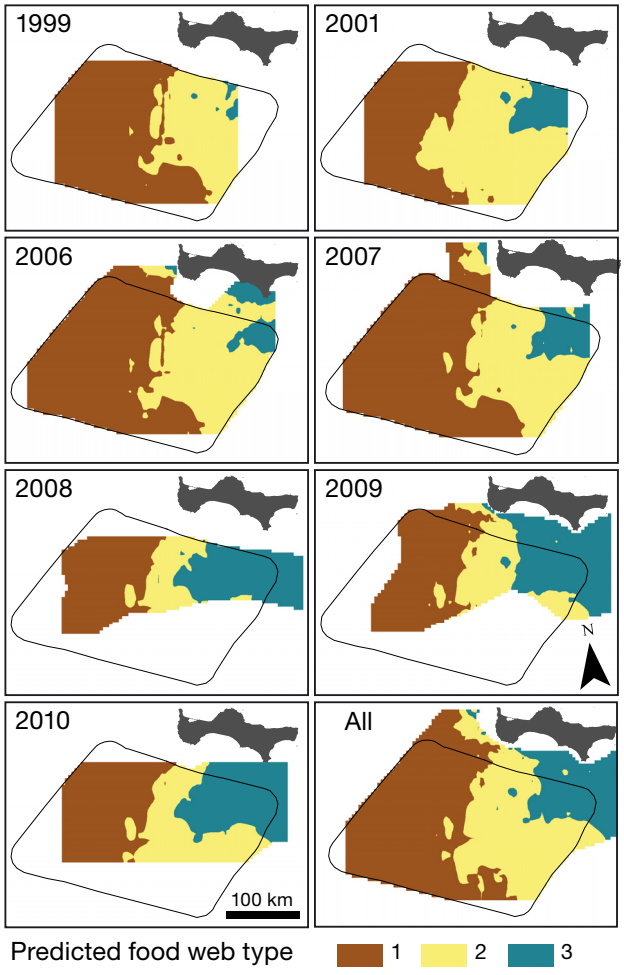

Fig. 8. Predicted spatial patterns of 3 benthic food web types associated with levels of longer-term organic carbon (LTOC) in the top 5 cm of sediments (Lovvorn et al. 2018a) south of St. Lawrence Island in the Bering Sea, based on equations for each year of sampling and for all years combined (Table 3). Type 1 (>23 g C m^{-2}) favors deposit-feeders, Type 2 is intermediate, and Type 3 (<9 g C m^{-2}) is dominated by filter-feeders

4. DISCUSSION

Due to differences in landscape patterns of bathymetry and hydrography, efforts to estimate the distributions of benthic communities from ocean circulation models will likely be regionally specific, with different factors exerting variable influence (cf. our results vs. Rand et al. 2018 for the Barrow Canyon area in the Chukchi Sea). However, within regions having a gradient of food web types, such as the gently sloping, soft bottoms of the Pacific Arctic shelves (Grebmeier et al. 2015b, Lovvorn et al. 2018a), we have shown that it is possible to model existing and potential spatial patterns based on only 1 or a few integrative variables (Lovvorn et al. 2016, 2018a; see also Weinert et al. 2016).

With the caveat that patterns of LTOC north of St. Lawrence Island were based on only 2 years of sampling, our results suggest that protecting only portions of this area would be adequate to sustain food web Type 3, but not Type 1 and perhaps not Type 2 in all years. Implementing protections for a broad area south of the island would sustain both Types 1 and 2 but would likely not be adequate to sustain Type 3 in all years. For types in each region that occur inconsistently among years, a number of longer-lived taxa could likely persist through intermittent periods of too much or too little accumulation of sediment OC by adjusting their metabolic rates, growth, or reproductive output. However, a series of

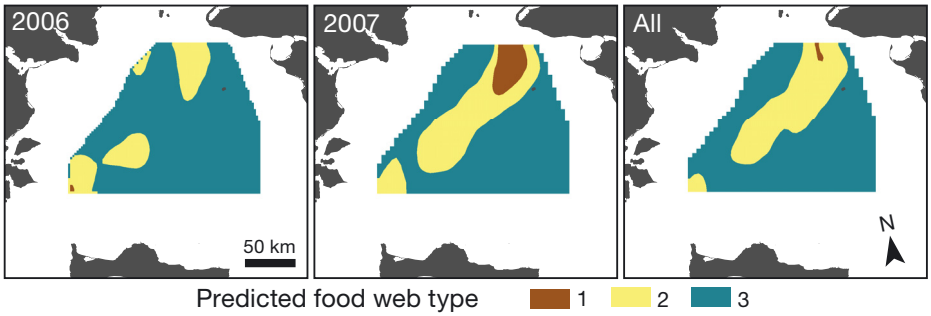

Fig. 9. Predicted spatial patterns of 3 food web types associated with levels of longer-term organic carbon (LTOC) in the top 5 cm of sediments (Lovvorn et al. 2018a) in the Chirikov Basin north of St. Lawrence Island in the Bering Sea, based on equations for each year of sampling and for all years combined (Table 4). Type 1 (>23 g C m^{-2}) favors deposit-feeders, Type 2 is intermediate, and Type 3 (<9 g C m^{-2}) is dominated by filter-feeders

such years in succession might greatly reduce or eliminate components of the food web important to upper-level predators, such as deposit-feeding bivalve taxa that achieve extraordinary densities in highly organic sediments (important to sea ducks), or filter-feeding ampeliscid amphipods that favor less organic sediments (important to gray whales). For long-term planning, a broad area south of the island as well as a substantial area north of the island would need to be included in plans to conserve a complement of these major food web types in all years.

4.1. Hindcasting vs. forecasting

In the northern Bering Sea, the more effective approach to projecting probable future distributions of LTOC and associated food web types differed between the 2 study areas. South of St. Lawrence Island, by far the best predictor was bathymetry, which will not change appreciably over relevant time scales. Annual variations in coverage of different food web types in Fig. 8 appear to be mainly expansions and contractions of areal extent over a stable bathymetric gradient, perhaps due to changes in total primary production. Core areas most likely to persist in all years, such as the area of Type 3 in 1999 and 2006 (Fig. 8), are of greatest conservation priority. In this subregion, hydrographic models may be of limited value for predicting future patterns of LTOC once patterns of LTOC with depth are identified over a series of years that encompass a wide range of conditions. In contrast, in the Chirikov Basin, patterns of LTOC were mainly a function of near-bottom currents. However, because those currents varied widely in timing and spatial pattern among years, a regression including only a few years would likely not capture important annual differences or identify areas where particular food web types were available in all years. Hindcasts over a series of years that include a wide range of conditions are more likely to encompass areas where different food web types would persist under a shifting climate (cf. Figs. 8 & 9).

4.2. Alternative approaches for delineating assemblages and food web types

Because different taxa have unique environmental affinities, it has been argued that the distribution of each taxon should be analyzed separately at multiple scales rather than as part of an integrated assemblage of species with similar distributions (Silberberger et al. 2019). Other studies have also focused on responses of individual taxa to gradients of environmental factors to predict assemblages found in a given area (Gogina et al. 2010, Reiss et al. 2011). Variations among taxa in dispersal ability and settlement preferences support the logic of this individual-species approach (Corte et al. 2018, Silberberger et al. 2019). However, in addition to their independent tolerances, component species usually interact directly or indirectly with other species on whose distributions they depend (Lovvorn et al. 2016). Accordingly, many studies have found recognizable assemblages of species that consistently co-occur (Van Hoey et al. 2004, Garcia et al. 2011, Lovvorn et al. 2015a). For example, the spacing of our sampling stations (Fig. 1) generally corresponded to the mesoscale (20 km) of Silberberger et al. (2019) in which the spatial pattern of different epifaunal taxa did not correspond to any environmental driver they examined. This result suggests that species interactions among epifauna, or between epifauna and their prey or predators, may have played an important role.

Moreover, marine spatial planning often requires delineation and partitioning of space among competing and sometimes incompatible conservation and human uses (Douvere 2008). Stipulating spatial limits to differing types or intensities of human use based on varying individual gradients of an array of component species will often be impractical. It may also be financially infeasible to sample at scales ranging from many tens of kilometers to single kilometers over large areas to assess diverse taxa whose distributions may each vary at different scales. By using an ocean circulation model to predict values of a dominant biotic driving variable (sediment LTOC) at 4- to 5-km resolution, our approach allows estimates of the spatial patterns of both community composition and food web function based on reasonable scales of field sampling.

For highly mobile predators, important habitats have also been delineated based on radiotelemetry (e.g. Citta et al. 2018). Such areas have been further characterized via resource selection functions, which compare environmental variables and even suites of available prey between locations that are used vs. not used by animals carrying satellite transmitters (Dickson & Smith 2013, Beatty et al. 2016). These approaches are compelling because they are based on direct measurements of animals in the field. However, they do not account for suitable areas that are unused in unsaturated habitat, especially by species with much reduced populations (Camaclang et al. 2015). They also do not consider social interactions (such as persistent flocking) or lack of omniscience about the locations and quality of all habitats, which may vary among years. Both of these factors can result in under-use of suitable areas or even use of low-quality areas at the time the animals' locations are recorded. These shortcomings can be overcome by larger sample sizes over longer periods. Nevertheless, mechanistic understanding of both habitat dependencies and the factors that generate those habitats is needed to estimate spatial patterns of suitable areas under altered environmental conditions.

4.3. Importance of episodic disturbances

Prediction of the benthic food web type that typically occurs at a given location can be confounded by major disturbances (Harris 2012). Storms on the Bering Sea shelf occasionally produce waves about 200 m long and 10 m high, which can disrupt soft-bottom sediments at water depths of at least 90 m (Sharma 1972). Benthic feeding by walruses and gray whales, which can occur in large concentrations, can also restructure sea floor communities at a local scale (Klaus et al. 1990). After major benthic faunal mortality, disturbance effects depend on differences among taxa in the magnitude, timing, and distance of planktonic or post-settlement dispersal, followed by interactions among colonizing species (Strasser & Günther 2001, Corte et al. 2018). Our samples of macrobenthos retained by a 1 mm sieve do not represent newly settled planktonic or drifting early stages of benthic fauna, but only older individuals that have survived post-settlement conditions or perhaps post-settlement dispersal. The 3 major food web types in the northern Bering Sea shared many of the same taxa; the types differed mainly in consistency of occurrence and relative biomass of the major deposit- or filter-feeding species, and of fish or invertebrate predators on those species (Lovvorn et al. 2015a, 2018a). Regardless of possible disturbances, assemblage structure in our region appeared to be strongly affected by LTOC levels that annually integrated a range of variables favoring certain herbivores, microbivores, and associated predators, either in choice of settlement location or interactions with other food web components.

4.4. Effects of ice on patterns of primary production, LTOC, and associated food webs

At local scales of only tens of kilometers in the northern Bering Sea, the spatial distribution of sediment chlorophyll often does not match patterns of primary production in the upper water column (Lovvorn et al. 2013). However, at larger scales, the areal extent and melt chronology of sea ice do affect the total magnitude of primary production (Cooper et al. 2012, Brown & Arrigo 2013, Grebmeier et al. 2018), and may thereby alter LTOC and associated benthic communities. The overall east to west increase in LTOC (Fig. 4) and total benthic biomass (Grebmeier et al. 2006) south of St. Lawrence Island may be partly explained by temporal and spatial patterns of ice break-up and resulting open water for bloom formation (Feng et al. 2018, unpubl. data). However, in our studies, neither chlorophyll concentrations integrated throughout the water column, nor surface sediment chlorophyll measured during or shortly after the peak of the spring bloom, corresponded well to LTOC at more local scales (Fig. 3; Lovvorn et al. 2013).

Why might spatial patterns of chlorophyll measured near the top of the water column from satellites be poorly related to local patterns of benthic communities? For our 2 Bering Sea study areas and in the

northern and southern Chukchi Sea, total biomass of benthic macrofauna was highly correlated with sediment total OC ($r^2 = 0.89$). However, sediment total OC had much lower correlation with surface sediment chl *a* (freshly settled microalgae) ($r^2 = 0.22$) (Grebmeier et al. 2018). A collection of benthic deposit-feeders (3 bivalve species, a polychaete, and a brittle star) in our Bering Sea study areas did ingest diatoms freshly settled from the spring bloom; however, stable isotope and fatty acid biomarkers indicated that the diatoms generally were not assimilated, and that these invertebrates instead subsisted mainly on bacteria consuming longer-term sediment organic matter (Lovvorn et al. 2005, North et al. 2014). Similar findings have been reported for the Antarctic Peninsula region and the Chukchi Sea (Mincks et al. 2008, McTigue & Dunton 2014). Moreover, evaluating the spatial pattern of total primary production in the water column is complicated by the inability of satellite sensors to measure chlorophyll at depths exceeding 5–6 m when chlorophyll maxima commonly occur at 20 to 40 m, and by the very limited temporal and spatial coverage of chlorophyll depth profiles measured from ships during relatively infrequent research cruises (Lovvorn et al. 2015a). Based on our results here and in earlier studies, models to link satellite data on ice-influenced, near-surface primary production to local patterns of soft-bottom assemblages must consider the redistribution of settled phytodetritus and organic sediments in relation to depth and near-bottom currents (Fig. 3; Lovvorn et al. 2013).

4.5. Links to climate models

Contemporary global climate models (general circulation models, GCMs) typically have atmospheric horizontal resolutions of 1–3° (60–180 nautical miles, n miles) and oceanic resolutions of 1–2° (60–120 n miles) (Stock et al. 2011, Wang et al. 2012, Hermann et al. 2016). However, global models have been downscaled to link with regional ocean circulation models having horizontal resolution as fine as 4–13 n miles (Ådlandsvik 2008, Mathis et al. 2013, Hermann et al. 2016).

In the Bering Sea, such downscaled climate models have been used to predict the biomass of all benthic infaunal taxa combined. These models were based on standard equations applied uniformly to all taxa to estimate their metabolic response to temperature and their relative ingestion of small and large phytoplankton and detritus (Gibson & Spitz 2011, Hermann et al. 2016). However, metabolic responses to temperature and reliance on filter-feeding vs. deposit-feeding often vary substantially among taxa of benthic invertebrates, and responses to temperature tend to be highly nonlinear below 5°C for which few measurements are available (see the Supplementary Material in Lovvorn et al. 2015a). Nevertheless, these models did recognize that changes in the amount, type, and quality of food are an important component of climate change effects on benthic communities.

Alternatively, climate-driven changes in dispersion of different benthic invertebrates have been modeled by projecting geographic shifts in the temperature and salinity ranges at which different taxa are currently observed to occur (Weinert et al. 2016). That approach does not directly account for trophic interactions among taxa that can strongly alter responses to environmental change (Lovvorn et al. 2018a). Moreover, many empirical studies indicate that climate-driven changes in organic matter inputs are far more important than temperature in altering metabolic rates, growth, and trophic interactions (Clarke 1988, Ahn et al. 2003, Eriksson Wiklund et al. 2009, Carroll et al. 2009).

Stock et al. (2011) suggested that better predictions of climatic impacts on living marine resources require improved understanding of mechanisms that link biotic components to climate, and better representation of those mechanisms in more holistic models. Toward this end, we identified sediment LTOC as a variable that integrates many mechanisms that determine food web structure and function in soft sediments of the northern Bering Sea. Based on studies that revealed LTOC as the principal carbon input to the benthic communities (Lovvorn et al. 2005, 2015a, North et al. 2014), we established that the 3 major recognizable assemblages occurred along a gradient of LTOC (Lovvorn et al. 2018a). When food web models developed for these assemblages were subjected to shifts in sediment LTOC spanning the range of values observed in the field, simulated changes in the food webs were similar to those observed (Lovvorn et al. 2016). In this paper we have related sediment LTOC, an integrative mechanistic variable driving food web structure and function, to bathymetry and hydrographic patterns predicted from a regional ocean circulation model. The ROMS framework has been used in several cases for downscaling from global climate models (Ådlandsvik 2008, Hermann et al. 2016), and our work provides a path for that subsequent step.

We were interested in delineating food webs at scales small enough to be relevant to the movements of benthic bird and mammal predators (Lovvorn et al.

2009, 2014, Dickson & Smith 2013, Citta et al. 2018). At such small scales (tens of kilometers), the spatial patterns of conditions favoring different food web types can vary appreciably among years, and our results show that simulations over a number of years are needed to identify areas where particular food web types persist (cf. Figs. 8 & 9). Once the model parameters and their ranges that are most related to different food web types are identified for particular regions, hindcasts under a variety of climate change scenarios can be generated to aid in long-term spatial planning.

Finally, we note that our analyses do not directly consider planktonic larval or post-settlement dispersal in estimating the distributions of benthic assemblage types. Current-driven dispersal processes have often been emphasized in planning spatial arrangements among units within reserve networks (Ross et al. 2017). As noted earlier, the 3 major types of benthic food web in the northern Bering Sea contain many of the same species, but differ substantially in consistency of occurrence and relative biomass of those species (Lovvorn et al. 2015a, 2018a). Consequently, our focus has been on areas in which a recurring supply of dispersing recruits is modified by post-settlement processes to yield differential occurrence and relative biomass of taxa among benthic food web types. Nevertheless, predictions of temperature, salinity, and current patterns make the approach presented here well-suited for simulating dispersal patterns under different climatic conditions (Parada et al. 2010).

Acknowledgements. Funding was provided by the US National Science Foundation, Office of Polar Programs grants ARC 1263051 to J.R.L.; ARC-0454454 to J.R.L., J.M.G., and L.W.C.; ARC-0802290 and 1702456 to J.M.G. and L.W.C.; and North Pacific Research Board project 713 to J.R.L.; S.L.D. and K.S.H. were supported by North Pacific Research Board project 1302, National Science Foundation grant OPP-1603116, and Bureau of Ocean Energy Management grant M15AC00011. C. A. North, J. M. Kolts, X. Cui, and L. Beaven provided important field, laboratory, and analytical support.

LITERATURE CITED

Ådlandsvik B (2008) Marine downscaling of a future climate scenario for the North Sea. Tellus A Dyn Meteorol Oceanogr 60:451–458

Ahn IY, Surh J, Park YG, Kwon H and others (2003) Growth and seasonal energetics of the Antarctic bivalve *Laternula elliptica* from King George Island, Antarctica. Mar Ecol Prog Ser 257:99–110

Beatty WS, Jay CV, Fischbach AS, Grebmeier JM, Taylor RL, Blanchard AL, Jewett SC (2016) Space use of a dominant Arctic vertebrate: effects of prey, sea ice, and land on Pacific walrus resource selection. Biol Conserv 203:25–32

Blanchard AL, Feder HM (2014) Interaction of habitat complexity and environmental characteristics with macrobenthic community structure at multiple spatial scales in the northeastern Chukchi Sea. Deep Sea Res II 102:132–143

Born EW, Rysgaard S, Ehlme G, Sejr M, Acquarone M, Levermann N (2003) Underwater observations of foraging free-living Atlantic walruses (*Odobenus rosmarus rosmarus*) and estimates of their food consumption. Polar Biol 26:348–357

Brower AA, Ferguson MC, Schonberg SV, Jewett SC, Clarke JT (2017) Gray whale distribution relative to benthic invertebrate biomass and abundance: northeastern Chukchi Sea 2009–2012. Deep Sea Res II 144:156–174

Brown ZW, Arrigo KR (2013) Sea ice impacts on spring bloom dynamics and net primary production in the eastern Bering Sea. J Geophys Res Oceans 118:43–62

Camaclang AE, Maron M, Martin TG, Possingham HP (2015) Current practices in the identification of critical habitat for threatened species. Conserv Biol 29:482–492

Carroll ML, Johnson BJ, Henkes GA, McMahon KW, Voronkov A, Ambrose WG, Denisenko SG (2009) Bivalves as indicators of environmental variation and potential anthropogenic impacts in the southern Barents Sea. Mar Pollut Bull 59:193–206

Citta JJ, Lowry LF, Quakenbush LT, Kelly BP and others (2018) A multi-species synthesis of satellite telemetry data in the Pacific Arctic (1987–2015): overlap of marine mammal distributions and core use areas. Deep Sea Res II 152:132–153

Clarke A (1988) Seasonality in the Antarctic marine environment. Comp Biochem Physiol B Comp Biochem 90: 461–473

Clement JL, Maslowski W, Cooper LW, Grebmeier JM, Walczowski W (2005) Ocean circulation and exchanges through the northern Bering Sea — 1979–2001 model results. Deep Sea Res II 52:3509–3540

Cooper LW, Grebmeier JM, Larsen IL, Egorov VG, Theodorakis C, Kelly HP, Lovvorn JR (2002) Seasonal variation in sedimentation of organic materials in the St. Lawrence Island polynya region, Bering Sea. Mar Ecol Prog Ser 226:13–26

Cooper LW, Janout M, Frey KE, Pirtle-Levy R, Guarinello M, Grebmeier JM, Lovvorn JR (2012) The relationship between sea ice break-up, water mass variation, chlorophyll biomass, and sedimentation in the northern Bering Sea. Deep-Sea Res II 65-70:141–162

Corte GN, Gonçalves-Souza T, Checon HH, Siegle E, Coleman RA, Amaral ACZ (2018) When time affects space: dispersal ability and extreme weather events determine metacommunity organization in marine sediments. Mar Environ Res 136:139–152

Curchitser EN, Haidvogel DB, Hermann AJ, Dobbins EL, Powell TM, Kaplan A (2005) Multi scale modeling of the North Pacific Ocean: assessment and analysis of simulated basin scale variability (1996–2003). J Geophys Res 110:C11021

Danielson S, Aagaard K, Weingartner T, Martin S, Winsor P, Gawarkiewicz G, Quadfasel D (2006) The St. Lawrence polynya and the Bering shelf circulation: new observations that test the models. J Geophys Res Oceans 111:C09023

Danielson S, Curchitser E, Hedstrom K, Weingartner T, Stabeno P (2011) On ocean and sea ice modes of variability in the Bering Sea. J Geophys Res Oceans 116:C12034

Danielson S, Weingartner T, Aagaard K, Zhang J, Woodgate R (2012) Circulation on the central Bering Sea shelf, July 2008 to July 2010. J Geophys Res Oceans 117:C10003

Danielson SL, Weingartner TJ, Hedstrom KS, Aagaard K, Woodgate R, Curchitser E, Stabeno PJ (2014) Coupled wind-forced controls of the Bering-Chukchi shelf circulation and the Bering Strait throughflow: Ekman transport, continental shelf waves, and variations of the Pacific-Arctic sea surface height gradient. Prog Oceanogr 125: 40–61

Danielson SL, Dobbins EL, Jakobsson M, Johnson MA, Weingartner TJ, Williams WJ, Zarayskaya Y (2015) Sounding the northern seas. EOS Earth Space Sci News

Danielson SL, Hedstrom KS, Weingartner TJ (2016) The southern Chukchi Sea's response to variations in Bering Sea circulation pathways. Proj 1302 Final Rep. North Pacific Research Board, Anchorage, AK

Danielson SL, Eisner L, Ladd C, Mordy CW, Sousa L, Weingartner TJ (2017) A comparison between late summer 2012 and 2013 water masses, macronutrients, and phytoplankton standing crops in the northern Bering and Chukchi Seas. Deep Sea Res II 135:7–26

De la Torriente A, González-Irusta JM, Aquilar R, Fernández-Salas LM, Punzón A, Serrano A (2019) Benthic habitat modelling and mapping as a conservation tool for marine protected areas: a seamount in the western Mediterranean. Aquat Conserv 29:732–750

Denisenko SG, Denisenko NV, Lehtonen KK, Andersin AB, Laine AO (2003) Macrozoobenthos of the Pechora Sea (SE Barents Sea): community structure and spatial distribution in relation to environmental conditions. Mar Ecol Prog Ser 258:109–123

Dickson DL, Smith PA (2013) Habitat used by common and king eiders in spring in the southeast Beaufort Sea and overlap with resource exploration. J Wildl Manag 77: 777–790

Douvere F (2008) The importance of marine spatial planning in advancing ecosystem-based sea use management. Mar Policy 32:762–771

Eriksson Wiklund AK, Dahlgren K, Sundelin B, Andersson A (2009) Effects of warming and shifts of pelagic food web structure on benthic productivity in a coastal marine system. Mar Ecol Prog Ser 396:13–25

Feng Z, Ji R, Ashjian CJ, Zhang J, Campbell RG, Grebmeier JM (2018) Physical and biological coupling processes in the St. Lawrence Island Polynya, northern Bering Sea: observational and modeling synthesis. 2018 Ocean Sciences Meeting, Portland, OR

Garcia C, Chardy P, Dewarumez JM, Dauvin JC (2011) Assessment of benthic ecosystem functioning through trophic web modelling: the example of the eastern basin of the English Channel and the Southern Bight of the North Sea. Mar Ecol 32(Suppl 1):72–86

Gawarkiewicz G, Haney JC, Caruso MJ (1994) Summertime synoptic variability of frontal systems in the northern Bering Sea. J Geophys Res 99(C4):7617–7625

Gibson GA, Spitz YH (2011) Impacts of biological parameterization, initial conditions, and environmental forcing on parameter sensitivity and uncertainty in a marine ecosystem model for the Bering Sea. J Mar Syst 88:214–231

Gogina M, Glockzin M, Zettler ML (2010) Distribution of benthic macrofaunal communities in the western Baltic Sea with regard to near-bottom environmental parameters. 2. Modelling and prediction. J Mar Syst 80:57–70

Gormley KSG, Porter JS, Bell MC, Hull AD, Sanderson WG (2013) Predictive habitat modelling as a tool to assess the change in distribution and extent of an OSPAR priority habitat under an increased ocean temperature scenario: consequences for marine protected area networks and management. PLOS ONE 8:e68263

Grebmeier JM, Cooper LW (2014) PacMARS Sediment Chlorophyll-a, Version 1.0. UCAR/NCAR - Earth Observing Laboratory, http://dx.doi.org/10.5065/D6W9576K

Grebmeier JM, Cooper LW (2016) PacMARS Surface Sediment Parameters, Version 2.0. UCAR/NCAR - Earth Observing Laboratory, http://dx.doi.org/10.5065/D6416V3G

Grebmeier JM, McRoy CP (1989) Pelagic-benthic coupling on the shelf of the northern Bering and Chukchi Seas. III. Benthic food supply and carbon cycling. Mar Ecol Prog Ser 53:79–91

Grebmeier JM, Cooper LW, Feder HM, Sirenko BI (2006) Ecosystem dynamics of the Pacific-influenced northern Bering and Chukchi Seas in the Amerasian Arctic. Prog Oceanogr 71:331–361

Grebmeier JM, Bluhm BA, Cooper LW, Danielson SL and others (2015a) Ecosystem characteristics and processes facilitating persistent macrobenthic biomass hotspots and associated benthivory in the Pacific Arctic. Prog Oceanogr 136:92–114

Grebmeier JM, Bluhm BA, Cooper LW, Denisenko SG, Iken K, Kędra M, Serratos C (2015b) Time-series benthic community composition and biomass and associated environmental characteristics in the Chukchi Sea during the RUSALCA 2004–2012 Program. Oceanography 28: 116–133

Grebmeier JM, Frey KE, Cooper LW, Kędra M (2018) Trends in benthic macrofauna populations, seasonal sea ice persistence, and bottom water temperatures in the Bering Strait region. Oceanography 31:136–151

Harris PT (2012) On seabed disturbance, marine ecological succession and applications for environmental management: a physical sedimentological perspective. In: Li MZ, Sherwood CR, Hill PR (eds) Sediments, morphology and sedimentary processes on continental shelves. IAS Special Publication 44. International Association of Sedimentologists, West Sussex, p 387–404

Harris PT, Macmillan-Lawler M, Kullerud L, Rice JC (2018) Arctic marine conservation is not prepared for the coming melt. ICES J Mar Sci 75:61–71

Hermann AJ, Gibson GA, Bond NA, Curchitser EN and others (2016) Projected future biophysical states of the Bering Sea. Deep Sea Res II 134:30–47

Kissling WD, Dormann CF, Groeneveld J, Hickler T and others (2012) Towards novel approaches to modelling biotic interactions in multispecies assemblages at large spatial extents. J Biogeogr 39:2163–2178

Klaus D, Oliver JS, Kvitek RG (1990) The effects of gray whale, walrus, and ice gouging disturbance on benthic communities in the Bering Sea and Chukchi Sea, Alaska. Natl Geogr Res 6:470–484

Kösters F, Winter C (2014) Exploring German Bight coastal morphodynamics based on modelled bed shear stress. Geo-Mar Lett 34:21–36

Le Hir P, Monbet Y, Orvain F (2007) Sediment erodability in sediment transport modelling: Can we account for biota effects? Cont Shelf Res 27:1116–1142

Lovvorn JR, Cooper LW, Brooks ML, De Ruyck CC, Bump JK, Grebmeier JM (2005) Organic matter pathways to zooplankton and benthos under pack ice in late winter and open water in late summer in the north-central Bering Sea. Mar Ecol Prog Ser 291:135–150

Lovvorn JR, Grebmeier JM, Cooper LW, Bump JK, Richman SE (2009) Modeling marine protected areas for threat-

ened eiders in a climatically changing Bering Sea. Ecol Appl 19:1596–1613
Lovvorn JR, Raisbeck MF, Cooper LW, Cutter GA and others (2013) Wintering eiders acquire exceptional Se and Cd burdens in the Bering Sea: physiological and oceanographic factors. Mar Ecol Prog Ser 489:245–261
Lovvorn JR, Anderson EM, Rocha AR, Larned WW and others (2014) Variable wind, pack ice, and prey dispersion affect the longer-term adequacy of protected areas for an Arctic sea duck. Ecol Appl 24:396–412
Lovvorn JR, Jacob U, North CA, Kolts JM, Grebmeier JM, Cooper LW, Cui X (2015a) Modeling spatial patterns of limits to production of deposit-feeders and ectothermic predators in the northern Bering Sea. Estuar Coast Shelf Sci 154:19–29
Lovvorn JR, Rocha AR, Jewett SC, Dasher D, Oppel S, Powell AN (2015b) Limits to benthic feeding by eiders in a vital Arctic migration corridor due to localized prey and changing sea ice. Prog Oceanogr 136:162–174
Lovvorn JR, North CA, Kolts JM, Grebmeier JM, Cooper LW, Cui X (2016) Projecting the effects of climate-driven changes in organic matter supply on benthic food webs in the northern Bering Sea. Mar Ecol Prog Ser 548:11–30
Lovvorn JR, North CA, Grebmeier JM, Cooper LW, Kolts JM (2018a) Sediment organic carbon integrates changing environmental conditions to predict benthic assemblages in shallow Arctic seas. Aquat Ecol 28:861–871
Lovvorn JR, Rocha AR, Mahoney AR, Jewett SC (2018b) Sustaining ecological and subsistence functions in conservation areas: eider habitat and access by Native hunters along landfast ice. Environ Conserv 45:361–369
Mathis M, Mayer B, Pohlmann T (2013) An uncoupled dynamical downscaling for the North Sea: method and evaluation. Ocean Model 72:153–166
McHenry J, Steneck RS, Brady DC (2017) Abiotic proxies for predictive mapping of nearshore benthic assemblages: implications for marine spatial planning. Ecol Appl 27: 603–618
McTigue ND, Dunton KH (2014) Trophodynamics and organic matter assimilation pathways in the northeast Chukchi Sea, Alaska. Deep Sea Res II 102:84–96
Mincks SL, Smith CR, Jeffreys RM, Sumida PYG (2008) Trophic structure on the West Antarctic Peninsula shelf: detritivory and benthic inertia revealed by $\delta^{13}C$ and $\delta^{15}N$ analysis. Deep Sea Res II 55:2502–2514
Nelson CH, Johnson KR (1987) Whales and walruses as tillers of the sea floor. Sci Am 256:112–117
North CA, Lovvorn JR, Kolts JM, Brooks ML, Cooper LW, Grebmeier JM (2014) Deposit-feeder diets in the Bering Sea: potential effects of climatic loss of sea ice-related microalgal blooms. Ecol Appl 24:1525–1542
Oliver JS, Slattery PN (1985) Destruction and opportunity on the sea floor: effects of gray whale feeding. Ecology 66: 1965–1975
Oliver JS, Slattery PN, O'Connor EF, Lowry LF (1983) Walrus, *Odobenus rosmarus*, feeding in the Bering Sea: a benthic perspective. Fish Bull 81:501–512
Parada C, Armstrong DA, Ernst B, Hinckley S, Orensanz JM (2010) Spatial dynamics of snow crab (*Chionoecetes opilio*) in the eastern Bering Sea — putting together pieces of the puzzle. Bull Mar Sci 86:413–437
Pautzke C (2005) The challenge of protecting fish habitat through the Magnuson–Stevens Fishery Conservation and Management Act. Am Fish Soc Symp 41:19–40
Pirtle-Levy R, Grebmeier JM, Cooper LW, Larsen IL (2009) Chlorophyll *a* in Arctic sediments implies long persistence of algal pigments. Deep Sea Res II 56:1326–1338
Puls W, Sundermann J (1990) Simulation of suspended sediment dispersion in the North Sea. In: Cheng RT (ed) Residual currents and longer-term transport. Springer-Verlag, New York, NY, p 356–372
Rand K, Logerwell E, Bluhm BA, Chenelot H, Danielson S, Iken K, Sousa L (2018) Using biological traits and environmental variables to characterize two Arctic epibenthic invertebrate communities in and adjacent to Barrow Canyon. Deep Sea Res II 152:154–169
Reiss H, Cunze S, König K, Neumann H, Kröncke I (2011) Species distribution modelling of marine benthos: a North Sea case study. Mar Ecol Prog Ser 442:71–86
Ross RE, Nimmo-Smith WAM, Howell KL (2017) Towards 'ecological coherence': assessing larval dispersal within a network of existing Marine Protected Areas. Deep Sea Res I 126:128–138
Rutgers van der Loeff MM, Meyer R, Rudels B, Rachor E (2002) Resuspension and particle transport in the benthic nepheloid layer in and near Fram Strait in relation to faunal abundances and ^{234}Th depletion. Deep Sea Res I 49: 1941–1958
Sharma GD (1972) Graded sedimentation on Bering Shelf. Int Geol Congr Sess 24:262–271
Sheffield G, Grebmeier J (2009) Pacific walrus (*Odobenus rosmarus divergens*): differential prey digestion and diet. Mar Mamm Sci 25:761–777
Silberberger MJ, Renaud PE, Buhl-Mortensen L, Ellingsen IH, Reiss H (2019) Spatial patterns in sub-Arctic benthos: multiscale analysis reveals structural differences between community components. Ecol Monogr 89:e01325
Steenbeek J, Coll M, Gurney L, Melin F, Hoepffner N, Buszowski J, Christensen V (2013) Bridging the gap between ecosystem modeling tools and geographic information systems: driving a food web model with external spatial-temporal data. Ecol Model 263:139–151
Stock CA, Alexander MA, Bond NA, Brander KM and others (2011) On the use of IPCC-class models to assess the impact of climate on living marine resources. Prog Oceanogr 88:1–27
Strasser M, Günther CP (2001) Larval supply of predator and prey: temporal mismatch between crabs and bivalves after a severe winter in the Wadden Sea. J Sea Res 46: 57–67
Thomsen L, Flach E (1997) Mesocosm observations of fluxes of particulate matter within the benthic boundary layer. J Sea Res 37:67–79
Van Hoey G, Degraer S, Vincx M (2004) Macrobenthic community structure of soft-bottom sediments at the Belgian Continental Shelf. Estuar Coast Shelf Sci 59:599–613
Wang M, Overland JE, Stabeno P (2012) Future climate of the Bering and Chukchi Seas projected by global climate models. Deep-Sea Res II 65-70:46–57
Weinert M, Mathis M, Kröncke I, Neumann H, Pohlmann T, Reiss H (2016) Modelling climate change effects on benthos: distributional shifts in the North Sea from 2001 to 2099. Estuar Coast Shelf Sci 175:157–168
Welschmeyer NA (1994) Fluorometric analysis of chlorophyll *a* in the presence of chlorophyll *b* and phaeopigments. Limnol Oceanogr 39:1985–1992

Appendix

Table A1. List of independent variables regressed against longer-term organic carbon (LTOC) in sediments sampled during 18–28 May 2007 south of St. Lawrence Island and 29 May to 3 June 2007 in the Chirikov Basin. Winter was defined as October through April, and the prior 5 yr period was 2002–2007. Flow vectors and resultant flow speeds are from the bottom layer of the ROMS model (extending ~1.5 m above the sea floor)

Bathymetric depth from either PAROMS, ARDEM, or shipboard bathymetric data
Drainage area, based on depths from PAROMS
Slope of sea floor, based on depths from PAROMS for each 19 km^2 pixel
Salinity (from PAROMS)
Mean and SD among all months in the prior 5 yr
Mean and SD among preceding months during the current winter
Individual means for each of the prior 12 mo
Month-to-month change during the prior year
Water temperature (from PAROMS)
Mean and SD among all months in prior 5 yr
Mean and SD among preceding months during the current winter
Individual means for each of the prior 12 mo
Month-to-month change during the prior year
Distance to nearest location with current flow speed >5 cm s^{-1} (1983–2007)
East–west and north–south flow vectors (from PAROMS)
Mean and SD among all months in the prior 5 yr
Mean and SD among all months during the prior 5 winters
Mean and SD among preceding months during the current winter
Individual means for each of the prior 12 mo
Resultant flow speed (from PAROMS)
Mean and SD among all months (1983–2007)
Mean and SD among all months during the prior 5 winters
Mean and SD among preceding months during the current winter
Individual means for each of the prior 12 mo
Month-to-month change during the prior year

Editorial responsibility: Romuald Lipcius, Gloucester Point, Virginia, USA

Submitted: May 20, 2019; Accepted: October 9, 2019
Proofs received from author(s): November 28, 2019